EXPERIMENTALLY TESTING MODEL-PREDICTED CRYSTALLIZATION TRENDS OF THE LUNAR HIGHLANDS MG-SUITE. M. F. Balemian-Spencer[1,2,3] and T. C. Prissel[1]; [1]Lunar and Planetary Institute, Universities Space Research Association, Houston, TX 77058, [2]Scripps College, Claremont, CA 91711, [3]Pomona College Geology Department, Claremont, CA 91711. (contact: tprissel@lpi.usra.edu).

Introduction: The Lunar Highlands Mg-suite is among the most ancient (~4.3 Ga) and pristine lunar sample suites, thus, its petrogenesis informs us about the earliest period of lunar magmatism [1]. Current models suggest that the Mg-suite formed either by (1) partial melting of a shallow-level hybridized source region, or (2) plagioclase contamination into a MgO-rich melt; both models imply a marked presence of pink-spinel troctolites (PST) [2,3,4,5]. However, PSTs comprise less than 2% of the troctolites found within the Mg-suite's natural data collection, by mass [6].

As an explanation for the volumetrically minor PSTs, we propose that the Mg-suite experienced plagioclase contamination, as the second model suggests, but with contamination restricted to the narrow margins of magma-wallrock interactions [2,7]. The remaining 98% of Mg-suite troctolites (without pink spinel), therefore, being formed from crystallization of the larger, uncontaminated regions of the same primitive melt [8].

SPICE (Simulating Planetary Igneous Crystallization Environments) MATLAB codes MAGPOX and MAGFOX model liquid lines of descent for our hypothesis. Model outcomes demonstrate that primitive melts can explain Fe-norites and redefine which lithologies comprise the Mg-suite (Fig. 1) [8]. This study tests model-predicted crystallization trends and modeling software through a series of experiments.

Experimental Methods:

Experimental composition. The primary melt (PM) compositional powder used in this research is taken from [8] and is derived from a terrestrial primitive analogue, komatiite. PM composition was attained by iteratively increasing Mg# (Mg# = Fo# = cation fraction of Mg/(Mg+Fe)*100) until the bulk composition is in equilibrium with Fo95 (Mg# ~95). Fo95 represents the most primitive natural troctolite sample [2].

Experimental process. Conditioned PM powders were pressed (dry) into pellets (~100-200 mg) and fastened to 0.25 mm diameter Re-wire loops. The low FeO-loss (less than 15%) with Re-wire at the experimental conditions explored here makes it ideal for this study [9]. Fastened pellets are then glassed at various temperatures (Table 1) within a Deltech 1 atm vertical gas-mixing furnace (CO-CO_2 continuous flow) at IW (Fe-FeO buffer).

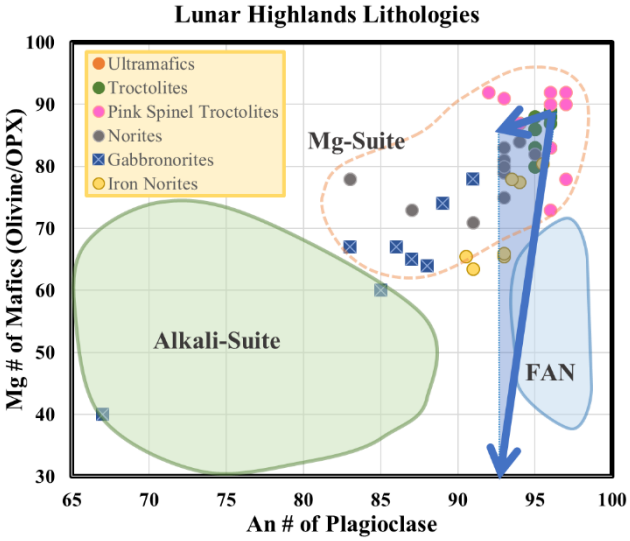

Figure 1. *Lunar Highlands natural data samples plotted with respect to the Mg# of the dominant mafic silicate phase and the An# of the plagioclase present in the sample. Arrows follow model-predicted crystallization trends and composition range for the Mg-suite (highlighted in blue).*

Analytical methods. Experimental glass analyses were performed using a JEOL 8530 and CAMECA SX 100 Electron Microprobe Analyzer (ARES), with a defocused beam, accelerating voltage of 15kV, and beam current of 20nA. Mineral phases were analyzed with a focused beam. For fractional crystallization steps (Table 1; PMb-series), PM8 glass serves as the target composition for synthetic PMb2. The PMb-series then follows the process outlined above.

Results: Experimental glass is visually and chemically homogenous (Table 1). Glass in the simulated fractional crystallization step (PMb2) is within 2σ standard deviation of the target glass composition (PM8).

Olivine in experiments PM1, PM8, PM9, and PMb1 range in size from 10-200 µm. Most olivine is euhedral, however, olivine in experiment PMb1 has a subhedral, skeletal texture. Additionally, some olivine crystals in experiments PM1, PM9, and PMb1 have a pitted texture on exposed faces. Mg# ranges from 93.8-87.1 for the experiments reported here.

Exp. Name	Target Comp.		PM1		PM9		PMb 2		PM8		PMb 1	
Temp (˚C)	1563*		1550		1350		1300		1250		1200	
Phases	-		Glass & Ol		Glass & Ol		Glass		Glass, Ol, & Sp		Gl, Ol, OPX, & Sp	
n	-		30		11		42		37		117	
Oxide	**Wt %**	**S.D.**	**Wt %**	**S.D.**	**Wt %**	**S.D.**	**Wt %**	**S.D.**	**Wt %**	**S.D.**	**Wt %**	**S.D.**
SiO_2	45.93	-	46.1	0.3	50.1	0.4	51.5	0.5	51.8	0.7	52.3	0.5
TiO_2	0.30	-	0.30	0.03	0.51	0.03	0.63	0.05	0.6	0.1	0.67	0.05
Al_2O_3	7.00	-	8.1	0.1	12.0	0.2	14.6	0.4	14.8	0.1	15.4	0.6
Cr_2O_3	0.50	-	0.50	0.03	0.57	0.05	0.40	0.07	0.38	0.04	0.25	0.05
FeO	8.90	-	10.4	0.1	9.8	0.2	8.0	0.2	8.0	0.2	7.9	0.3
MnO	0.20	-	0.20	0.02	0.27	0.04	0.21	0.06	0.24	0.04	0.21	0.06
MgO	31.5	-	28.5	0.2	16.9	0.2	11.8	0.2	11.9	0.1	9.8	0.4
CaO	5.50	-	6.20	0.08	9.7	0.2	11.7	0.2	11.7	0.1	12.5	0.2
Na_2O	0.15	-	0.03	0.02	0.04	0.02	0.22	0.03	0.08	0.02	0.22	0.03
K_2O	0.02	-	BDL	-	BDL	-	0.03	0.02	BDL	-	0.03	0.02
Total	100.00	-	100.39	-	99.89	-	99.09	-	99.50	-	99.28	-
Mg #	86.3	-	83.0	0.2	75.6	0.4	72.5	0.6	72.7	0.4	68.7	0.7

Table 1. *Glass data from experiments PM1, PM8, PM9, PMb1, PMb2, and "target composition" (taken from [8]) organized by decreasing temperature. "Phases" information indicates minerals and melt presence (Gl=glass, Ol=olivine, Sp=chromium spinel, and OPX=orthopyroxene), while "n" indicates the number of data points collected for a given experiment. Reported Mg# is taken from glass analyses. Standard deviation is reported in 2σ. *Predicted liquidus temperature for "target composition."*

Pyroxene in experiment PMb1 (first fractional step) has lengths ranging from 600-1,000 µm and widths ranging from 125-145µm. The pyroxene has a pitted texture much like the olivine crystals in experiments PM1, PM9, and PMb1. Mg#=87.2 (± 0.5) for the pyroxene analyzed. Pyroxene in experiment PMb1 is of low-Ca variety with an average CaO weight percent of 2.5 ± 0.2.

Trace amounts of chromium spinel present in experiments PM8 and PMb1 have not yet been analyzed. Data will be collected in the near future.

Testing for equilibrium. The Fe-Mg olivine/orthopyroxene-melt equilibrium exchange coefficient ($K_D = [Fe/Mg]^{ol/opx} * [Mg/Fe]^{liquid}$) for olivine ranges from 0.32-0.34, and for orthopyroxene, $K_D = 0.32 \pm 0.02$. These results are consistent with previous experimental studies, [10,11,12,].

Discussion: Experimentally determined liquid lines of descent align well with model results. Experiments PM1, PM9, and PM8 follow equilibrium liquid lines of descent closely, while PMb1 (first fractional step) plots closer to fractional trends. Thus, SPICE program codes MAGPOX and MAGFOX accurately predict the experimental outcomes within the reported experimental range.

Olivine compositions also closely follow modeled data and show that primitive melt compositions can crystallize large quantities of olivine while retaining high Mg#, contrary to previous petrogenetic models [6]. Experimental data therefore supports conclusions drawn by [8] that Mg-suite troctolites can be explained by crystallization of primitive mantle melts, whereas PST can be explained through interaction with lunar crust.

Because experimental data so closely resembles model data, further experimentation is warranted to test plagioclase crystallization and composition. Future work will continue exploring the experimental fractional crystallization methods.

Establishing an accurate petrogenetic narrative of the Mg-suite will provide a deeper understanding of the lunar magma ocean, timing and global extent of cumulate mantle overturn, and can potentially redefine current differentiation trends [8].

References: [1] R.W. Carlson et al. (2014) *Phil. Trans. Royal Soc. A, 372.* [2] T.C. Prissel et al. (2016) *Am. Min., 101*, 1624-1635. [3] J. Longhi et al. (2009) *Geochim. Cosmochim. Acta, 74,* 784-798. [4] S.M. Elardo et al (2011), *Geochim. Cosmochim. Acta, 75,* 3024-3045. [5] J. Gross and A. Treiman (2011), *J. Geophys. Res., 116.* [6] C.K. Shearer et al. (2015) *Am. Min., 100,* 294-325. [7] T.C. Prissel et al. (2014) *Earth Planet. Sc. Lett., 403,* 144-156. [8] T.C. Prissel and J. Gross (2019) *50th LPSC,* Abstract #3106. [9] A. Borisov and J.H. Jones (1999) *Am. Min., 84,* 1528-1534. [10] K. Mibe et al. (2006) *Geochim. Cosmochim. Acta, 70,* 757-766. [11] J. Filiberto et al. (2011) *Earth Planet. Sc. Lett., 304,* 527-537. [12] A.K. Matzen et al., (2011) *J. Pet., 52,* 1243-1263.